



# Research on blast resistance performance of petrochemical industry shelter

Meng Gu <sup>a,b</sup>, Hanxiang Wang <sup>a,\*</sup>, Anfeng Yu <sup>b</sup>, Haozhe Wang <sup>b</sup>, Guoxin Chen <sup>b</sup>  
Xiaodong Ling <sup>b</sup>

<sup>a</sup> College of Mechanical and Electronic Engineering, China University of Petroleum (East China), Qingdao, 266580, China

<sup>b</sup> SINOPEC Research Institute of Safety Engineering Co., Ltd., Qingdao, 266104, China

\*Corresponding author: wanghx@upc.edu.cn

**Abstract.** Explosion accidents in petrochemical enterprises often caused heavy casualties and economic losses. However, most existing buildings close to production facilities were not designed to withstand explosion loads. Steel shelter could be used to replace the low strength buildings which cannot meet explosion resistance requirements. In this study, the loads on each side of the shelter were calculated based on the explosion shock wave and the size of the shelter. The structural response of shelter main frame was studied by finite element simulation. It was found that the blast wave reflected on the front wall of the shelter, which was subjected to the maximum pressure load. Only a few members of the main frame entered the stage of plastic deformation, and the support angle and maximum stress met the requirements of explosion resistance. The research results could provide an effective method for the blast resistant reconstruction of petrochemical buildings.

**Keywords:** Explosion wave; Blast resistance shelter; Structural response; Finite element simulation

## 1 Introduction

Most of the materials involved in petrochemical plants were flammable and explosive hydrocarbon liquids and gases. Once the leakage of hazardous materials occurred, it could cause fire and explosion accidents, resulting in heavy casualties and economic losses[1-3]. Related statistics showed that 75% of casualties in petrochemical plant accidents were related to building damage caused by vapor cloud explosions[4]. However, most of the existing buildings closed to the production facilities only considered the fire protection requirements and were not designed to withstand blast loadings. The feasibility, economy and construction period of the reinforcement of the existing building should be analyzed according to the original building structure. For existing buildings with low resistance to progressive collapse, after retrofitting the infill walls with fiber-reinforced composite materials[5] and polyurea[6], it was still necessary to comprehensively reinforce the load-bearing structure. When the renovation project was

© The Author(s) 2024

Q. Gao et al. (eds.), *Proceedings of the 2024 7th International Conference on Structural Engineering and Industrial Architecture (ICSEIA 2024)*, Atlantis Highlights in Engineering 30,

[https://doi.org/10.2991/978-94-6463-429-7\\_27](https://doi.org/10.2991/978-94-6463-429-7_27)

long and costly, new blast resistant shelters could be used to replace such existing buildings[7]. Compared with newly constructed cast-in-place reinforced concrete blast resistant buildings, steel blast resistant shelters had the advantages of high blast resistance, short construction period, and minimal impact on the normal production of enterprises, which could significantly reduce the cost of improving blast resistance.

In this paper, the blast loading of the shelter of a petrochemical enterprise was calculated according to the parameters of incident shock wave, and the main frame was analyzed by 3D finite element method. The research results could provide a new solution for the petrochemical buildings which were difficult to strengthen by conventional methods, and provide a reference for the research and application of steel structure shelters.

## 2 Blast loading

The operation room of an enterprise was adjacent to the liquefied hydrocarbon loading and unloading platform, which had the risk of fire and explosion. Field sampling and testing showed that the strength of masonry wall brick was lower than MU7.5 and the strength of mortar was lower than M5. Therefore, it was difficult and costly to carry out blast-resistant reinforcement for existing buildings. In order to reduce the risk of casualties in explosion accident, a new blast resistant steel structure shelter was proposed.

Based on quantitative risk assessment, it was determined that the peak incident overpressure ( $P_{so}$ ) of shock wave at the new shelter was 37.2 kPa, the positive pressure time ( $t_d$ ) was 57.7 ms. The design appearance size of the shelter was  $36 \times 6 \times 3.6$  m. The blast load of each side of a closed rectangular building can be calculated by the following formula[7].

(1) Front wall loading

$$P_r = (2 + 0.0073P_{so})P_{so} \quad (1)$$

$$t_e = (t_d - t_c) \frac{P_s}{P_r} + t_c \quad (2)$$

Where,  $P_r$  is peak reflected pressure;  $t_e$  is the duration of the equivalent triangle;  $P_s$  is stagnation pressure;  $t_c$  is the duration of the reflected overpressure effect.

(2) Side wall and roof loadings

$$P_a = C_e P_{so} + C_d q_o \quad (3)$$

$$t_r = L_1/U \quad (4)$$

Where,  $P_a$  is effective overpressure;  $C_e$  is reduction factor;  $q_o$  is Peak dynamic pressure;  $t_r$  is the rise-time of overpressure;  $L_1$  is the length of the structural element;  $U$  is Shock front velocity.

(3) Rear wall load

$$P_b = C_e P_{so} + C_d q_o \quad (5)$$

$$t_r = L_1/U \tag{6}$$

$$t_{rb} = S/U \tag{7}$$

Where,  $P_b$  is effective overpressure;  $t_{rh}$  is time of duration; S is clearing distance.

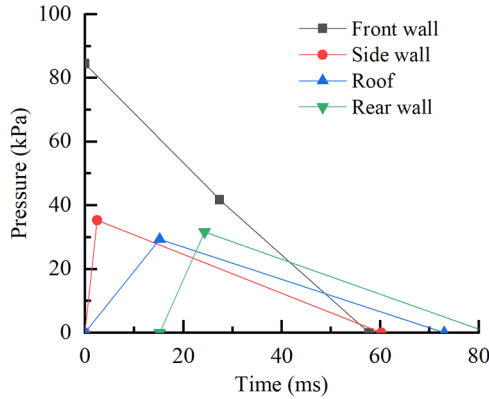


Fig. 1. Blast loading curves of the shelter

Combined with the relevant parameters of shock wave and shelter, the blast loading of the shelter walls and roof was calculated (Fig. 1).

### 3 Dynamic analysis of steel frame

In the explosion accident, the impact loading on the walls will be transferred to the main steel frame structure. The main frame was the key factor of blast resistant ability of building and its insufficient strength will lead to the overall collapse of the building. However, too small beam-column spacing of the main frame will increase the project cost and prolong the construction period. Therefore, 3D finite element methods was adopted to analyze the steel frame.

#### 3.1 Geometric model.

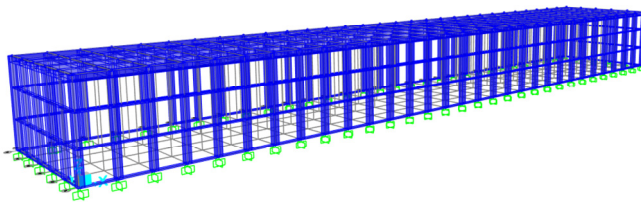
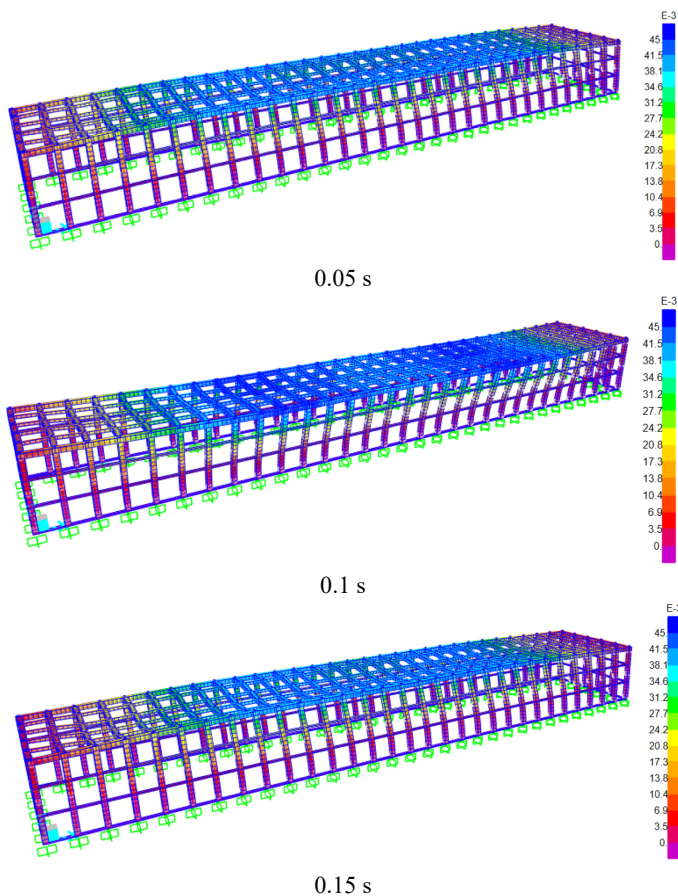


Fig. 2. Geometric model of shelter

As shown in Fig. 2, a full-scale geometric model of the shelter was established. Considering the mechanical properties and cost, the frame column and the main beam were made of 220 mm×220 mm×10 mm Q345 square steel. The height of the frame column was 3.6 m, and the span of the main beam was 6 m. The size of prefabricated blast resistant plate was 2400 mm× 1200 mm. In order to facilitate the installation of the 2.4 m wide blast resistant plate, the spacing between column to column and beam to beam was designed to be 1.2 m.

The steel shelter was anchored through the foundation, and the beam and column contact were welded. Therefore, rigid-joint connections were adopted between structural columns and foundations as well as structural parts. The line element was used to simulate the beam and column, and the shell element was used to simulate the blast resistant plate. The nonlinear time history analysis method was used to analyze the explosion load.

### 3.2 Simulation results and analysis.



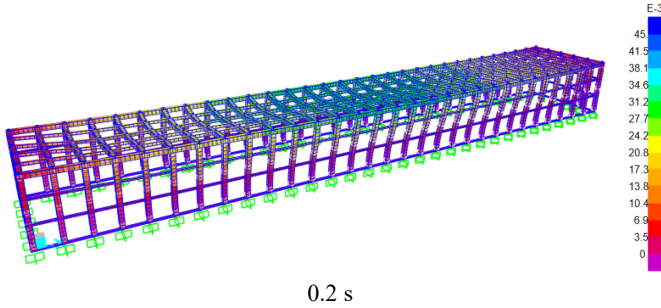


Fig. 3. Displacement of frame

The displacement of the frame under explosive load is shown in Fig. 3. Due to the highest load on the front wall and the large length of the shelter, the maximum displacement occurred at the top of the blast face of the shelter and the middle area of the roof. The maximum displacement of the steel column on the blast face was 45.3 mm. The maximum displacement of the column appeared at the top of the column, thus the deflection radius of the column adopted a column height of 3.6 m, and the calculated column support angle was  $0.72^\circ < 1^\circ$  (allowable value). The maximum deformation of the roof steel beam was 43.7 mm, and the maximum angle was  $0.83^\circ < 1^\circ$  (allowable value). The deformation of the beams and columns in the shelter met the safety requirement.

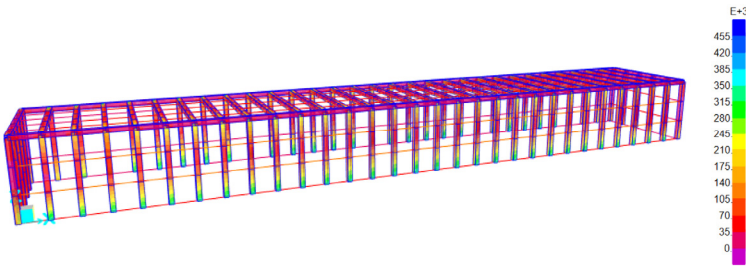


Fig. 4. Maximum stress of frame

The maximum stress of the frame during the structural response process is shown in Fig. 4, and the highest stress of the frame occurs on the blast face and the roof. The maximum stress of the blast face frame was 387 MPa, and the maximum stress of the roof frame was 369 MPa. For steel subjected to explosive load, the strength improvement coefficient was 1.1 and the dynamic improvement coefficient was 1.19 [8]. Therefore, the dynamic strength design value of Q345 steel is  $345 \text{ MPa} \times 1.1 \times 1.19 = 452 \text{ MPa}$ . The maximum stress in the shelter exceeded the static yield strength of the steel, but was less than the dynamic strength of the steel. Only a few members of the frame structure entered the plastic stage. Therefore, according to the stress analysis, the whole structure was still in the safe range.

## 4 Conclusions

(1) The blast wave reflected on the front wall of the shelter, which is subjected to the maximum pressure load. The maximum displacement and stress occur on the blast face and roof of the shelter.

(2) Finite element analysis shows that only a few members of the steel frame structure enter the plastic stage. The support angle and maximum stress meet the requirements of the specification requirements, and the whole steel frame is in the safe range.

(3) For petrochemical buildings that are difficult to be reinforced by conventional scheme, steel shelter can not only meet the requirements of explosion resistance safety, but also shorten the construction period, and reduce the cost of reconstruction. In subsequent research, multifunctional protection plates can be developed to match the steel frame, enabling the shelter to withstand both explosion waves and debris.

## References

1. Lees, F. (2012) *Lees' Loss Prevention in the Process Industries*. Elsevier Butterworth-Heinemann, Oxford. <https://doi.org/10.1016/B978-0-7506-7555-0.X5081-6>.
2. Chen, C., Khakzad, N., Reniers, G. (2020) Dynamic vulnerability assessment of process plants with respect to vapor cloud explosions. *Reliab. Eng. Syst. Safe.*, 200: 106934. <https://doi.org/10.1016/j.ress.2020.106934>.
3. Shamsuddin, D.S.N.A., Fekeri, A.F.M., Muchtar, A., Khan, F., Khor, B.C., Lim, B.H., Rosli, M.I., Takriff, M.S. (2023) Computational fluid dynamics modelling approaches of gas explosion in the chemical process industry: A review. *Process Saf. Environ. Prot.*, 170: 112-138. <https://doi.org/10.1016/j.psep.2022.11.090>.
4. Ministry of Construction of the PR China. (2014) *Code for design of petrochemical plant layout (GB 50984-2014)*. China Architecture and Building Press, Beijing. <https://www.nssi.org.cn/nssi/front/85181333.html>.
5. Anas, S.M., Alam, M. (2022) Performance of brick-filled reinforced concrete composite wall strengthened with C-FRP laminate(s) under blast loading. *Mater. Today: Proc.*, 65(1): 1-11. <https://doi.org/10.1016/j.matpr.2022.03.162>.
6. Wu, G., Ji, C., Wang, X., Gao, F., Zhao, C., Liu, Y., Yang, G. (2022) Blast response of clay brick masonry unit walls unreinforced and reinforced with polyurea elastomer. *Def. Technol.*, 18(4): 643-662. <https://doi.org/10.1016/j.dt.2021.03.004>.
7. ASCE. (2010) *Design of Blast-resistant Buildings in Petrochemical Facilities*. 2nd ed. ASCE Publications, Reston. <https://ascelibrary.org/doi/book/10.1061/9780784410882>.
8. Ministry of Housing and Urban-Rural Development of the PR China. (2022) *Standard for blast resistant design of buildings in petrochemical engineering (GB/T 50779-2022)*. China Planning Press, Beijing. <https://www.nssi.org.cn/nssi/front/118388403.html>.

**Open Access** This chapter is licensed under the terms of the Creative Commons Attribution-NonCommercial 4.0 International License (<http://creativecommons.org/licenses/by-nc/4.0/>), which permits any noncommercial use, sharing, adaptation, distribution and reproduction in any medium or format, as long as you give appropriate credit to the original author(s) and the source, provide a link to the Creative Commons license and indicate if changes were made.

The images or other third party material in this chapter are included in the chapter's Creative Commons license, unless indicated otherwise in a credit line to the material. If material is not included in the chapter's Creative Commons license and your intended use is not permitted by statutory regulation or exceeds the permitted use, you will need to obtain permission directly from the copyright holder.

